A General and Ultrafast Polishing Method with Truly-atomic Roughness

Yi Zhang[1,2,5], Yongjie Zhang[1,3,5], Kaixuan Gu[1], Linfeng Zhang[1], Yuanmin Zhu[4], Dianzi Liu[2] & Hui Deng[1,*]

[1]Department of Mechanical and Energy Engineering, Southern University of Science and Technology, Shenzhen, 518055, Guangdong, China

[2]School of Engineering, Faculty of Science, University of East Anglia, Norwich Research Park, Norwich NR4 7TJ, United Kingdom

[3]Department of Physics and Centre for Advanced 2D Materials, National University of Singapore, 2 Science Drive 3, Singapore 117551, Singapore

[4]Department of Materials Science and Engineering and Academy for Advanced Interdisciplinary Studies, Southern University of Science and Technology, Shenzhen, 518055, Guangdong, China

[5]These authors contributed equally: Yi Zhang and Yongjie Zhang

[*]Corresponding author.

Yi Zhang: zhangy8@mail.sustech.edu.cn

Yongjie Zhang: 12055005@mail.sustech.edu.cn

Kaixuan Gu: kaixuangu01@qq.com

Linfeng Zhang: 11930917@mail.sustech.edu.cn

Yuanmin Zhu: zhuym3@sustech.edu.cn

Dianzi Liu: Dianzi.Liu@uea.ac.uk

Hui Deng (Corresponding author): dengh@sustech.edu.cn

ABSTRACT

The advancement of science and technology is always accompanied by better manufacturing precision. Ideally, the highest precision for manufacturing a surface is truly-atomical flatness, which implies that all topmost surface-atoms are in a single layer of crystal face. However, almost no methods can achieve this surface with high efficiency at present. Herein, we present a method to fabricate large-scale true-atomically flat surface with ultrafast speed. Through the selective etching of surface atoms, our method can achieve the atomically flat surface with 0.05 nm *S*a roughness. It is notable that the polishing efficiency of our method is more than 1000 times higher than that of the conventional methods. We have demonstrated its generality on various single-crystal materials and obtained atomic roughness and ultrahigh polishing rate. This method has the potential to promote the mass-production of atomic-scale smooth surfaces, the application of third-generation semiconductor materials, and the innovation of advanced technologies.

TOC Graphic

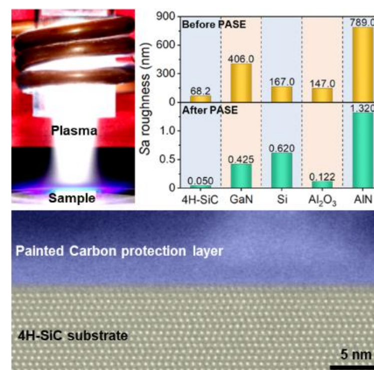

The advancement of manufacturing technologies is the foundation for the development of human civilization. From the craft-based manufacturing originated from over 4000 B.C. to the automatic production using machineries developed since the second industry revolution, the manufacturing precision has evolved from millimeter to micrometer and nanometer.[1] The developing of manufacturing technologies has always been chasing higher precision. Fang *et. al.* concludes the next phase of manufacturing as atomic and close-to-atomic scale manufacturing (ACSM) where the material removal, transformation, and addition are at atomic precision.[2] One of the important fields of ACSM is the manufacturing of an atomic-level surface, which means ideally all atoms within the surface are in the same layer of crystal plane. It is also known as the roughness limit of a surface in the field of applied physics.[3] Many state-of-the-art methods have been invented and developed to approach this goal. However, due to machine tools precision, volumetric removal with large amount of atoms, and low atomic manipulation efficiency, fabricating a large-scale surface with true-atomic-level precision is still challenging.[2]

Substantial effort has been devoted to obtaining an ultrasmooth surface with sub-nanometer roughness. Here we divided them into three categories: polishing method, exfoliation method, and tip-based method. The polishing method, which can fabricate relatively large-scale surface, can be categorized into mechanical method and hybrid-mechanical method. Mechanical method such as nano-grinding can avoid brittle fracture, as it can precisely control the grain depth cut to be equal or less than the critical depth of ductile removal.[4] To obtain a gentle loading pressure, magnetorheological fluid, fluid jet, and bonnet are often used to carry the abrasives.[5-7] Although this method can suppress microcracks and achieve sub-nanometer roughness, the formation of amorphous layer and subsurface damage is inevitable due to its nature of ductile deformation.[8] Hybrid-mechanical method can modify the sample surface via different mechanisms, which would make the material removal easier. The most commonly used surface modification approach is chemical reaction[9] and its derivative methods such as electrochemical[10] and photocatalytic reaction[11] are also adopted. However, these methods

generally show quite low efficiency for high-hardness and chemically inert materials. For both mechanical and hybrid-mechanical method, the ductile mode removal mechanism is eventually employed to understand the removal of surface material. It is impossible to confine the energy of each grain within the need to remove an atom and the exceeding force will always influence the subsurface atoms. Thus, mechanical-involved method is very difficult to achieve atomic precision. However, methods that are based on chemical etching and have no contact force with surface atoms can overcome this problem.

Exfoliation method are widely used for the fabrication of emergent 2D materials. The world's first piece of graphene was prepared through mechanical exfoliation and the investigation of many intrinsic properties, such as quantum Hall effect and superconductivity, are explored, based on graphene obtained by exfoliation method.[12-14] More recently, ion-intercalation, liquid exfoliation, electrochemically-assisted exfoliation, and Au-assisted exfoliation have greatly improved the usability of this method.[15-18] However, exfoliation method is only applicable for 2D materials, and it is still limited in lateral size, yield, and unexpected contaminations.

The most controllable method which can achieve true atomic precision is tip-based method. Using scanning tunneling microscopy (STM) or atomic force microscope (AFM), researchers can accurately manipulate a single atom.[19, 20] The removal of single atomic layer within a relatively large area of micrometer level has also been achieved by AFM-based mechanochemical reaction.[21] However, the manufacturing scale for tip-based methods is difficult to exceed one micrometer, which is still too small for device applications. Associated with the ultralow efficiency, high demand for expensive vacuum equipment, and highly skilled operators, applications of tip-based method are limited.

To fabricate a large-scale and true-atomically flat surface, advance the limitation of polishing technology, and facilitate the application of difficult-to-machine materials, we proposed the

plasma-based atom-selective etching (PASE) method. PASE is based on the selectively removal of surface atoms which constitute the surface roughness, and this is also the most direct way to reduce roughness without influencing the subsurface material.[22, 23] As shown in Figure 1a, the rough surface of single-crystal silicon carbide (4H-SiC) is formed by many atomic steps. The chemical activity of the atom on the step edge (SE-atom) and the step terrace (ST-atom) is different.[24, 25] Under the appropriate conditions (herein, we adopt plasma etching), the etching speed of SE-atoms can be much larger than that of ST-atoms, and thus etching can expend along the step edge, as shown in Figure 1b. When atom-selective etching is applied on all the SE-atoms on the surface, the atomic step edge can be quickly removed. As shown in Figure 1c and Movie S1, the atoms constituting surface roughness could be removed, and eventually a true-atomically flat surface is formed. The selective lateral etching can remove the unwanted atomic layers until all atoms achieve an equipotential state, which means all atoms are ideally located forming an integral crystal plane with truly-atomic flatness. Therefore, PASE can be regarded as a polishing technology that can achieve the ultimate surface roughness.

In addition to its most important feature of obtaining an atomic-level surface, PASE also has the characteristics of ultra-high efficiency and universal applicability to crystalline materials. As an etching process using atmospheric high-temperature and high-particle-density plasma, PASE shows ultra-fast polishing efficiency, compared with conventional polishing, exfoliation, and tip-based manipulation approaches. Unlike other existing precision surface manufacturing methods which could only start with raw surface with nano- or sub-nanometer roughness, this work would only take 5 min to directly polish a sliced 4H-SiC chip from *S*a roughness of around 68.2 nm to 0.05 nm. To achieve the atomic-scale smooth 4H-SiC surface, the conventional chemical mechanical polishing (CMP) generally needs more than 8 hours, as shown in Figure S1. Compared with exfoliation method and tip-based method, which can only generate atomic surfaces within micron level area, PASE is able to produce centimeter level atomic surface.

For the surface of any crystalline materials, unless it achieves the surface where surface atoms are regularly arranged with the same potential energy, there will be differences in the etching of atoms at different sites on the surface. Thus, PASE has the potential to be applied as a general polishing method for single-crystal materials. In this work, we have demonstrated the atomic scale polishing of 4H-SiC, GaN, Si, Al_2O_3, and AlN. PASE can greatly increase the polishing efficiency of many difficult-to-machine single-crystal materials and facilitate the application of next generation semiconductor materials. PASE could be easily applied on large size samples, if broad-scale and evenly plasma environment could be produced.

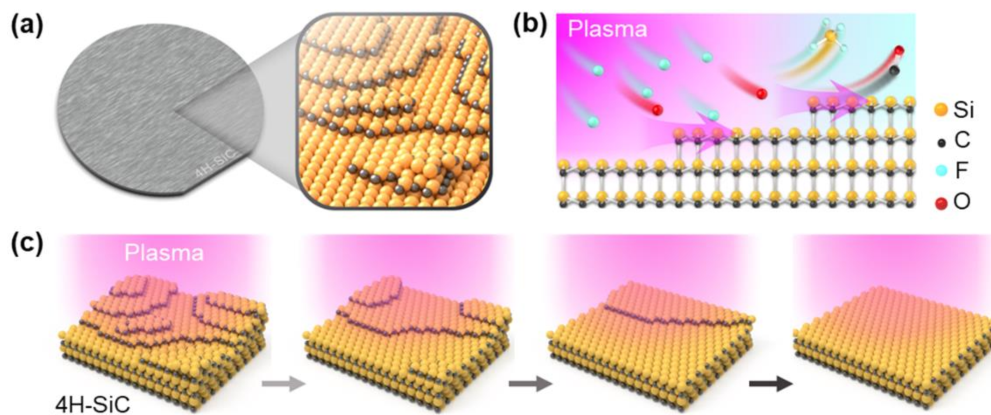

Figure 1. Mechanism of PASE for the polishing of 4H-SiC. (a) Schematic of a sliced 4H-SiC wafer and the atomic surface after magnification (right). (b) Schematic of the PASE process. (c) Schematic of the evolution of surface topography during PASE.

As a typical next-generation semiconductor and hard-to-machine material, 4H-SiC has been chosen to demonstrate the advancement of PASE method. We firstly adopted ab initio molecular dynamics (AIMD) simulation to analysis the etching process and explore the appropriate condition for the selective etching of surface atoms. As shown in Figures 2a and S2, the dissociate paths of step-edge Si atom (SE-Si) and step-terrace Si atom (ST-Si) under the irradiation of fluorine plasma are different. The calculated activation energies for SE-Si and ST-Si under 300 K are 0.25 and 0.54 eV respectively. According to Arrhenius equation, the etching of SE-Si should be 74435 times higher than that of ST-Si.[26] However, fluorine plasma

never shows such great lateral etching ability under room temperature in actual etching operation. We further extended the etching time to capture more details about PASE, as shown in Figures 2b and S3. After a few cycles of selective etching of SE-Si, we observed accumulation of amorphous carbon remained on the surface. Those amorphous carbon would hinder step edges and thus obstacle the following selectivity toward SE-Si. Thus, we introduced oxygen into plasma to remove the amorphous carbon. As shown in Figure 2c, the ability to remove absorbed carbon is weak under low temperature while higher temperature dramatically strengthens this ability.[27] Meanwhile, the absorption of O atoms on 4H-SiC surface can produce relatively loose Si-O structure, forming active sites that are easy to be etched. The amount of generated CO_X increases rapidly with the increase of temperature. Additionally, under 1500 K, carbon has not dissociated with the same amount of injecting F atoms, implying that O has much higher carbon removal ability than F. To sum up, the combination of F and O plasma can be used to realize atom-selective etching of 4H-SiC. F atoms serve as the main element to the selective etching of SE-Si and the etching speed is calculated to be 74435 times higher than that of ST-Si. O atoms can remove the accumulated amorphous carbon and expose the Si atoms behind. The carbon removal ability of O increases rapidly with temperature. Significantly, O would form loose Si-O structure on the surface, which can accelerate the etching process. At the macro level, the synergy of F and O could be an effective path for highly efficient etching of atomic steps on 4H-SiC. Therefore, the key point to achieve atom-selective etching of 4H-SiC is to modulate F and O atoms to an appropriate ratio and impose high temperature.

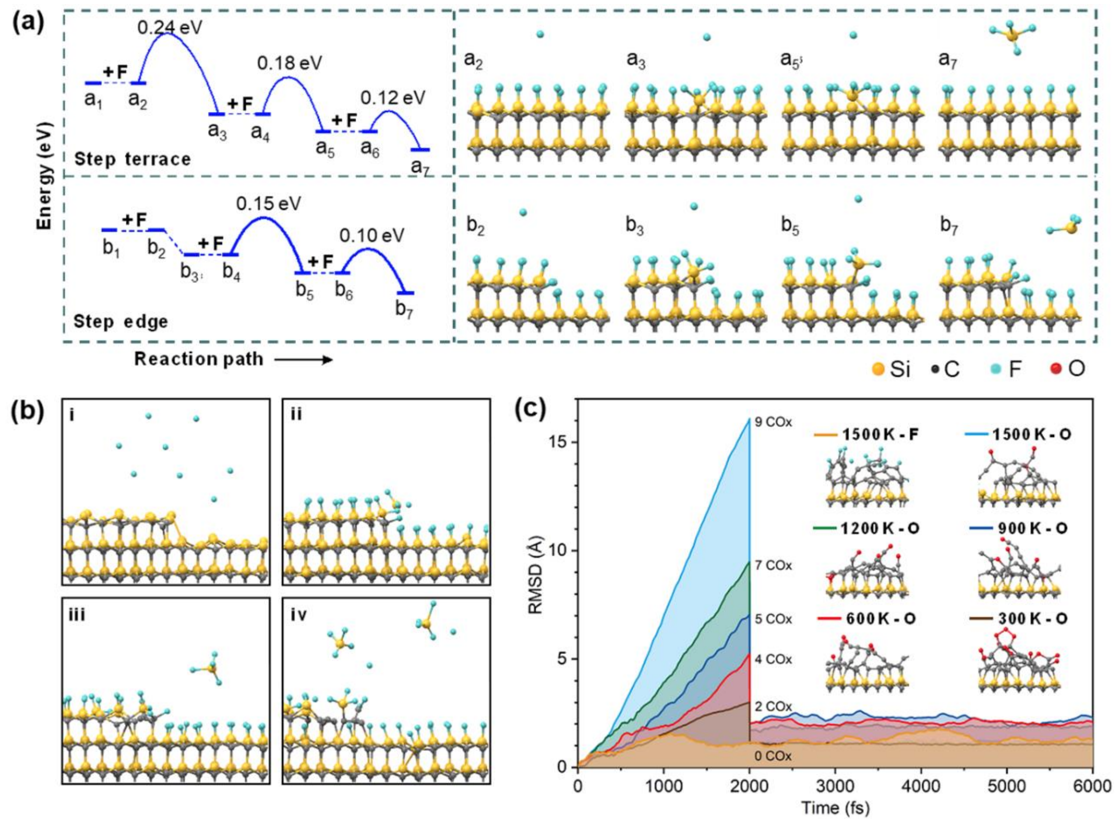

Figure 2. AIMD simulation of the PASE process for 4H-SiC. (a) Reaction paths of ST-atom and SE-atom. (b) An atomic step etched by F for multi times. (c) Root-mean-square deviation (RMSD) curve of the surface carbon layer etched by O atoms at 300-1500 K or by F atoms at 1500 K.

According to the simulation results, a dense and high temperature plasma that contains an appropriate proportion of F and O radicals is required for the PASE process. Herein, we utilize atmospheric pressure inductively coupled plasma (ICP) as the etchant to experimentally demonstrate the atomic-scale polishing ability of PASE. ICP torch can provide both high-temperature and high-radical-density plasma.[28] Meanwhile, as our plasma works under atmospheric pressure, which implies a low mean-free path, it would not introduce new damage caused by atomic bombardment commonly observed in low pressure and vacuum plasma.[29] The schematic experimental setup is shown in Figure 3a. The sample stage was made from alumina foam to maintain the high temperature of sample surface during PASE. A piece of quartz glass was placed on the foam to prevent powder contamination. During a typical polishing process, the ICP was ignited outside the substrate and then moved to the predefined location. The

temperature of the sample would quickly rise to over 1400 °C in 60 s (Figure 3b) and the heating rate is much higher than conventional furnaces or heating tables. The temperature can be regulated by modulating radio frequency (RF) power and stand-off distance (Figure S4). After the PASE process was conducted for the set duration, the RF power would be turned off and the 4H-SiC sample was cooled under the protection of Ar flow. Figure 3c shows the optical emission spectroscopy (OES) of ICP. After the addition of CF_4 into the plasma, strong CF_X (350-450 nm) peak and typical C_2 (450-570 nm) swan system can be observed clearly.[30-32] However, high concentration of C_2 could increase the surface absorption of carbon, which can hide the atomic step structure and impede the preferential edge etching effect. When oxygen is added, the intensity C_2 peak greatly decreased. Oxygen is also a highly electronegative gas, which can gain energy from energetic electrons and compete with CF_4; thus it can be seen that the intensity of CF_X peak is also reduced.[33] The peak at 777.6 nm represents the transitions of O atoms (3p5P→3s5S), suggesting that abundant O radicals could be used to remove the accumulated carbon layer.[34] The radical percentage can be controlled by modifying the input flow rate of CF_4 and O_2 (Figure S5). Therefore, this plasma source is considered to be able to meet the requirement for realization of PASE.

The surface morphology of etched 4H-SiC sample and the corresponding schematic diagram of surface profiles are shown in Figure 3d. The as-received surface of 4H-SiC, which is rough and seriously damaged, is pre-processed by slicing. Within 3 s, the amorphous layer on the surface has been quickly removed, as amorphous 4H-SiC contains more dangling bounds which should be easy to be etched. The surface processed by three-seconds etching already shows some small flat bottoms, which implies the significant role of lateral etching effect. After ten-seconds PASE, the surface demonstrates even more pronounced iconic flat bottoms, further conforming the lateral etching effect. With the etching going on, the flat bottom continually expended and finally combined together, forming an integral flat surface without any steps and terraces, which could be observed on the sample surface processed by PASE for 1 min. The

schematic diagram below and Movie S2 graphically show how the lateral etching can result in flat bottoms and eventually form an ultrasmooth surface. This set of samples can clearly prove that PASE can achieve lateral etching effect and polish the sample efficiently.

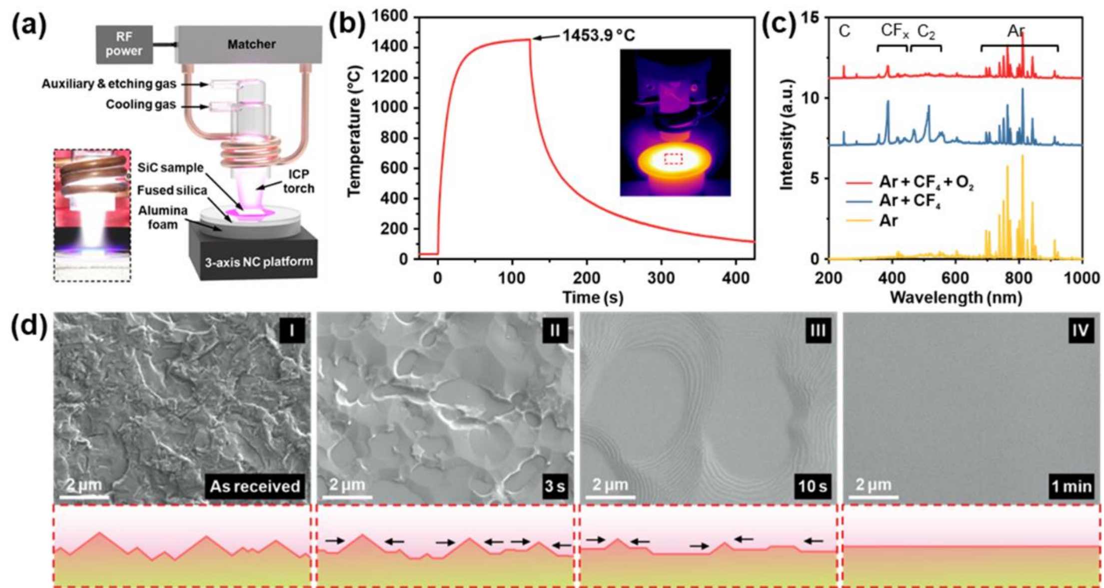

Figure 3. Experimental setup and PASE results of 4H-SiC. (a) Schematic diagram of experimental setup. (b) Sample surface temperature during PASE, where the whole operation time is 120 s. (c) OES results of the ICP torch with different reaction gases. (d) Scanning electron microscope (SEM) images of the sample surface and the corresponding schematic of the sample cross-section during PASE.

The selective etching effect in PASE was further confirmed by AFM. As shown in Figure 4a, within 10 s, selective etching sites with the flat bottom are formed on a rough sliced surface. And in 5 min, all atom steps disappear and the *S*a roughness decreases from around 68.2 nm to 0.05 nm. The power spectral density (PSD) curves in Figure 4b show an improvement of all spatial frequency, and meanwhile, it takes only 5 min to converge to the final PSD shown in Figure S6. The scanning transmission electron microscopy (STEM) result in Figure 4c shows the cross-sectional profile of the surface etched for 5 min, and a carbon layer was used to protect the topmost layer of atoms in focused ion beam (FIB) process.[35] It can be seen clearly that the surface layer is a integrate crystal plane surface without defects, missing atoms, and extra atoms.

The energy dispersive spectrometry (EDS) result in Figure 4d shows that only protective carbon paint layer (containing carbon and oxide) remains on the surface. To ensure that all the amorphous layer are from protective painting rather than the PASE polishing process, we have also prepared a FIB sample protected by electron beam evaporated Cr layer, and the result also indicates that the surface was well crystallized and atomically flat 4H-SiC (Figure S7). We obtained the lower magnification STEM images of 4H-SiC before and after PASE, and the results are shown in Figures 4e and 4f. The raw surface is heavily damages, and many strain patterns can be observed. The heavily twisted selected area electron diffraction (SAED) pattern also confirms the finding.[36] After PASE, the polished surface is visually uniform, and the typical SAED pattern of 11-20 zone-axis implies good crystallinity of the surface region,[31] suggesting that the SSD layer has been removed.

The PASE process is based on the selective etching of SE-atoms, which can be also interpreted as a much higher lateral etching speed compared with the vertical direction. This means the material removal rate (MRR) should be closely related to the surface roughness, as a higher roughness implies more exposed atomic step edges. The roughness and MRR are shown in Figure 4g. During the first-minute etching, the roughness rapidly decreased from 68.2 to 0.1 nm, then slowly reduced to 0.05 nm in 5 min, and finally remained at that roughness. The MRR also decreased from 58.1 μm/min to 31.7 μm/min in the first-minute PASE, and then converted to around 30 μm/min, which also proved the atom-selective etching mechanism. We compared PASE with many conventional and cut-edge methods, as shown in Figure 4h and Table S1. It can be found that PASE can reach the lowest roughness, while its efficiency is three orders of magnitude higher than that of these methods. Meanwhile, PASE is theoretically possible to achieve truly-atomic flatness, while other methods are not capable. PASE method breaks the rule that high MRR will result in rough surface; when MRR increase in PASE, the roughness remains almost the same with atomic level (Figure S8).

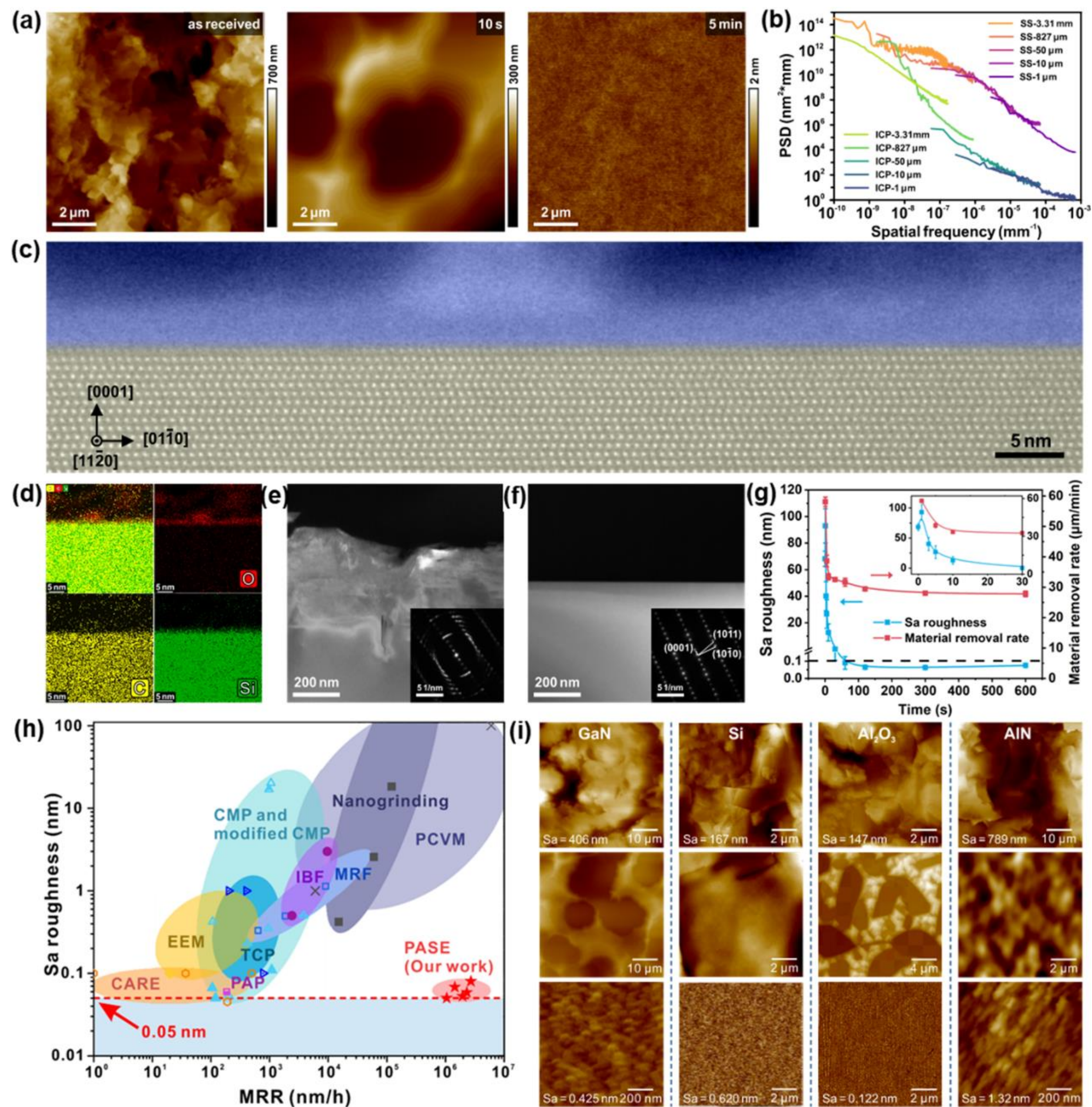

Figure 4. Ultrafast and atomic roughness polishing by PASE. (a) AFM images of 4H-SiC samples with different plasma durations. (b) PSD curves of 4H-SiC samples before and after PASE. (c) STEM image of the cross-section of 4H-SiC sample after PASE. (d) Element mapping results. (e, f) STEM images and SAED patterns of (e) as-received 4H-SiC sample and (f) polished 4H-SiC sample via PASE. (g) The roughness and MRR variations of 4H-SiC during PASE. (h) The comparison between PASE and other cutting-edge polishing methods. (i) The AFM images of various single-crystal materials polished by PASE.

We further demonstrated the general ability of PASE. Theoretically, all single-crystal materials could be polished by PASE. Herein, we explore the polishing of several typical difficult-to-machine materials, including GaN, Si, Al_2O_3, and AlN, via PASE, and the results are shown in Figure 4i. It is clear that all these materials have reached atomically flatness from sliced raw

surface in several minutes. Meanwhile, the localized flat bottom morphology has emerged in all samples during etching. These results suggest that PASE is practical in polishing wide range of single crystals. These results strongly demonstrate that PASE has the potential to be industrially utilized for the manufacturing of single-crystal wafers with truly-atomic flatness and ultrahigh efficiency with the level of μm/min.

PASE can produce true-atomically flat surface of single-crystal materials with ultrahigh efficiency. By controlling the plasma scale, uniformity, and temperature, it can be readily extended to process large size wafers.[37] PASE have the ability to substitute the lapping, mechanical polishing, and chemical mechanical polishing steps in conventional wafer manufacturing process, and greatly reduce the time cost. For instance, in this work, the polishing process of 4H-SiC has been reduced from over 8 hours to less than 10 min, which could reduce 12% of the manufacturing cost.[38] Thus, PASE will foster the application of devices based on them. The PASE process can be coupled with subsequent deposition or oxidation process, since the high temperature and gas phase environment needed for them are similar. Meanwhile, the ability of PASE to produce true-atomically flat surface will enable many cutting-edge applications that are possible with truly-atomic surfaces such as quantum chips, single-molecule electronics, and so forth.[39, 40]

Supporting Information

Materials and Method, Figures S1-S8, Table S1, and Movies S1 and S2.

Author Contributions

H.D. supervised the project. Y.Z. performed the experiment and characterization. Y.J.Z. and K.X.G contributed to the AIMD calculations and the mechanism analysis of PASE. L.F.Z. and Y.M.Z contributed to the TEM characterization. D.Z.L. contributed to useful

discussion. All the authors contributed to the writing of the manuscript. H.D. and Y.J.Z. revised the manuscript.

Notes

The authors declare no competing financial interest.

Acknowledgements

This project is supported by the National Natural Science Foundation of China (52005243, 52035009) and the Science and Technology Innovation Committee of Shenzhen Municipality (JCYJ20200109141003910, JCYJ20210324120402007). The authors acknowledge the assistance of SUSTech Core Research Facilities.

References

(1) Kalpakjian, S.; Schmid, S. R. *Manufacturing Engineering and Technology*; Pearson, 2001.

(2) Fang, F.; Zhang, N.; Guo, D.; Ehmann, K.; Cheung, B.; Liu, K.; Yamamura, K. Towards Atomic and Close-to-Atomic Scale Manufacturing. *Int. J. Extreme Manuf.* **2019**, *1*, 012001.

(3) Yu, J.; Namba, Y. Atomic Surface Roughness. *Appl. Phys. Lett.* **1998**, *73*, 3607-3609.

(4) Yin, L.; Pickering, J. P.; Ramesh, K.; Huang, H.; Spowage, A. C.; Vancoille, E. Y. J. Planar Nanogrinding of a Fine Grained WC-Co Composite for an Optical Surface Finish. *Int. J. Adv. Manuf. Technol.* **2005**, *26*, 766-773.

(5) Kordonski, W. I.; Jacobs, S. D. Magnetorheological Finishing. *Int. J. Mod. Phys. B* **1996**, *10*, 2837-2848.

(6) Walker, D. D.; Brooks, D.; Freeman, R.; King, A.; McCavana, G.; Morton, R.; Riley, D.; Simms, J. First Aspheric Form and Texture Results from a Production Machine Embodying the Precession Process. In *International Symposium on Optical Science and*

Technology, San Diego, CA, United States, 2001; Stahl, H. P., Ed.; Society of Photo-Optical Instrumentation Engineers: Vol. 4451, pp 267-276. DOI: 10.1117/12.453652.

(7) Booij, S. M. Nanometer Deep Shaping with Fluid Jet Polishing. *Opt. Eng.* **2002**, *41*, 1926-1931.

(8) Ngoi, B. K. A.; Sreejith, P. S. Ductile Regime Finish Machining - A Review. *Int. J. Adv. Manuf. Technol.* **2000**, *16*, 547-550.

(9) Aida, H.; Doi, T.; Takeda, H.; Katakura, H.; Kim, S.-W.; Koyama, K.; Yamazaki, T.; Uneda, M. Ultraprecision CMP for Sapphire, GaN, and SiC for Advanced Optoelectronics Materials. *Curr. Appl. Phys.* **2012**, *12*, S41-S46.

(10) Murata, J.; Yodogawa, K.; Ban, K. Polishing-Pad-Free Electrochemical Mechanical Polishing of Single-Crystalline SiC Surfaces Using Polyurethane-CeO_2 Core-Shell Particles. *Int. J. Mach. Tools Manuf.* **2017**, *114*, 1-7.

(11) Wang, W.; Zhang, B.; Shi, Y.; Zhou, J.; Wang, R.; Zeng, N. Improved Chemical Mechanical Polishing Performance in 4H-SiC Substrate by Combining Novel Mixed Abrasive Slurry and Photocatalytic Effect. *Appl. Surf. Sci.* **2022**, *575*, 151676.

(12) Novoselov, K. S.; Geim, A. K.; Morozov, S. V.; Jiang, D.; Zhang, Y.; Dubonos, S. V.; Grigorieva, I. V.; Firsov, A. A. Electric Field Effect in Atomically Thin Carbon Films. *Science* **2004**, *306*, 666-669.

(13) Zhang, Y.; Tan, Y. W.; Stormer, H. L.; Kim, P. Experimental Observation of the Quantum Hall Effect and Berry's Phase in Graphene. *Nature* **2005**, *438*, 201-204.

(14) Cao, Y.; Fatemi, V.; Fang, S.; Watanabe, K.; Taniguchi, T.; Kaxiras, E.; Jarillo-Herrero, P. Unconventional Superconductivity in Magic-Angle Graphene Superlattices. *Nature* **2018**, *556*, 43-50.

(15) Coleman, J. N.; Lotya, M.; O'Neill, A.; Bergin, S. D.; King, P. J.; Khan, U.; Young, K.; Gaucher, A.; De, S.; Smith, R. J.; et al. Two-Dimensional Nanosheets Produced by Liquid Exfoliation of Layered Materials. *Science* **2011**, *331*, 568-571.

(16) Fan, X.; Xu, P.; Zhou, D.; Sun, Y.; Li, Y. C.; Nguyen, M. A.; Terrones, M.; Mallouk, T. E. Fast and Efficient Preparation of Exfoliated 2H MoS_2 Nanosheets by Sonication-Assisted Lithium Intercalation and Infrared Laser-Induced 1T to 2H Phase Reversion. *Nano Lett.* **2015**, *15*, 5956-5960.

(17) Ambrosi, A.; Pumera, M. Exfoliation of Layered Materials Using Electrochemistry. *Chem. Soc. Rev.* **2018**, *47*, 7213-7224.

(18) Huang, Y.; Pan, Y. H.; Yang, R.; Bao, L. H.; Meng, L.; Luo, H. L.; Cai, Y. Q.; Liu, G. D.; Zhao, W. J.; Zhou, Z.; et al. Universal Mechanical Exfoliation of Large-Area 2D Crystals. *Nat. Commun.* **2020**, *11*, 2453.

(19) Hla, S. W. Atom-by-Atom Assembly. *Rep. Prog. Phys.* **2014**, *77*, 056502.

(20) Custance, O.; Perez, R.; Morita, S. Atomic Force Microscopy as a Tool for Atom Manipulation. *Nat. Nanotechnol.* **2009**, *4*, 803-810.

(21) Chen, L.; Wen, J.; Zhang, P.; Yu, B.; Chen, C.; Ma, T.; Lu, X.; Kim, S. H.; Qian, L. Nanomanufacturing of Silicon Surface with a Single Atomic Layer Precision via Mechanochemical Reactions. *Nat. Commun.* **2018**, *9*, 1542.

(22) Fang, Z.; Zhang, Y.; Li, R.; Liang, Y.; Deng, H. An Efficient Approach for Atomic-Scale Polishing of Single-Crystal Silicon via Plasma-Based Atom-Selective Etching. *Int. J. Mach. Tools Manuf.* **2020**, *159*, 103649.

(23) Deng, H.; Zhang, Y.; Liang, J.; Zhang, X. Surface Reconstruction of Sapphire at the Atomic Scale via Chemical-Physical Tuning of Atmospheric Plasma. *CIRP Ann. Manuf. Technol.* **2023**, *72*, 489-492.

(24) Shen, A.; Zou, Y.; Wang, Q.; Dryfe, R. A.; Huang, X.; Dou, S.; Dai, L.; Wang, S. Oxygen Reduction Reaction in a Droplet on Graphite: Direct Evidence That the Edge Is More Active Than the Basal Plane. *Angew. Chem. Int. Ed. Engl.* **2014**, *53*, 10804-10808.

(25) Shao, M.; Peles, A.; Shoemaker, K. Electrocatalysis on Platinum Nanoparticles: Particle Size Effect on Oxygen Reduction Reaction Activity. *Nano Lett.* **2011**, *11*, 3714-3719.

(26) Laidler, K. J. The Development of the Arrhenius Equation. *J. Chem. Educ.* **1984**, *61*, 494-498.

(27) Li, C. e.; Brown, T. C. Carbon Oxidation Kinetics from Evolved Carbon Oxide Analysis During Temperature-Programmed Oxidation. *Carbon* **2001**, *39*, 725-732.

(28) Tendero, C.; Tixier, C.; Tristant, P.; Desmaison, J.; Leprince, P. Atmospheric Pressure Plasmas: A Review. *Spectrochim Acta B* **2006**, *61*, 2-30.

(29) Bárdos, L.; Baránková, H. Plasma Processes at Atmospheric and Low Pressures. *Vacuum* **2008**, *83*, 522-527.

(30) Wang, R.; Zhang, C.; Liu, X.; Xie, Q.; Yan, P.; Shao, T. Microsecond Pulse Driven Ar/CF_4 Plasma Jet for Polymethylmethacrylate Surface Modification at Atmospheric Pressure. *Appl. Surf. Sci.* **2015**, *328*, 509-515.

(31) Zhang, Y.; Zhang, L.; Chen, K.; Liu, D.; Lu, D.; Deng, H. Rapid Subsurface Damage Detection of SiC Using Inductivity Coupled Plasma. *Int. J. Extreme Manuf.* **2021**, *3*, 035202.

(32) Resnik, M.; Zaplotnik, R.; Mozetic, M.; Vesel, A. Comparison of SF_6 and CF_4 Plasma Treatment for Surface Hydrophobization of Pet Polymer. *Mater.* **2018**, *11*, 311.

(33) Kimura, T.; Noto, M. Experimental Study and Global Model of Inductively Coupled CF_4/O_2 Discharges. *J. Appl. Phys.* **2006**, *100*, 063303.

(34) Zhou, R.-W.; Zhang, X.-H.; Zong, Z.-C.; Li, J.-X.; Yang, Z.-B.; Liu, D.-P.; Yang, S.-Z. Reactive Oxygen Species in Plasma Against *E. Coli* Cells Survival Rate. *Chin. Phys. B* **2015**, *24*, 085201.

(35) Schaffer, M.; Schaffer, B.; Ramasse, Q. Sample Preparation for Atomic-Resolution STEM at Low Voltages by FIB. *Ultramicroscopy* **2012**, *114*, 62-71.

(36) Yan, J.; Gai, X.; Harada, H. Subsurface Damage of Single Crystalline Silicon Carbide in Nanoindentation Tests. *J. Nanosci. Nanotechnol.* **2010**, *10*, 7808-7811.

(37) Lee, K.; Lee, Y.; Jo, S.; Chung, C.-W.; Godyak, V. Characterization of a Side-Type Ferrite Inductively Coupled Plasma Source for Large-Scale Processing. *Plasma Sources Sci. Technol.* **2008**, *17*, 015014.

(38) Reese, S. B.; Singh, A.; Zakutayev, A.; Akar, S.; Remo, T. Why Wideband Gap Needs Techno-Economics. In *2019 IEEE 7th Workshop on Wide Bandgap Power Devices and Applications (WiPDA)*, Raleigh, NC, USA, 29-31 October, 2019; IEEE: pp 337-341. DOI: 10.1109/WiPDA46397.2019.8998798.

(39) Joachim, C.; Martrou, D.; Rezeq, M.; Troadec, C.; Jie, D.; Chandrasekhar, N.; Gauthier, S. Multiple Atomic Scale Solid Surface Interconnects for Atom Circuits and Molecule Logic Gates. *J. Condens. Matter Phys.* **2010**, *22*, 084025.

(40) Wu, L.; Wang, A.; Shi, J.; Yan, J.; Zhou, Z.; Bian, C.; Ma, J.; Ma, R.; Liu, H.; Chen,

J.; et al. Atomically Sharp Interface Enabled Ultrahigh-Speed Non-Volatile Memory Devices. *Nat. Nanotechnol.* **2021**, *16*, 882-887.